Search for the rare decay $K^+ \to \pi^+ \gamma$

S. Adler,[1] M. Aoki,[6,*] M. Ardebili,[5] M. S. Atiya,[1] A. O. Bazarko,[5] P. C. Bergbusch,[6,8] E. W. Blackmore,[6] D. A. Bryman,[6,8] I-H. Chiang,[1] M. R. Convery,[5,†] M. V. Diwan,[1] J. S. Frank,[1] J. S. Haggerty,[1] T. Inagaki,[3] M. M. Ito,[5,‡] V. Jain,[1] S. Kabe,[3] M. Kazumori,[3,§] S. H. Kettell,[1] P. Kitching,[7] M. Kobayashi,[3] T. K. Komatsubara,[3] A. Konaka,[6] Y. Kuno,[3,‖] M. Kuriki,[3] T. F. Kycia,[1,¶] K. K. Li,[1] L. S. Littenberg,[1] J. A. Macdonald,[6] R. A. McPherson,[5,**] P. D. Meyers,[5] J. Mildenberger,[6] M. Miyajima,[2] N. Muramatsu,[3,§,††] T. Nakano,[4] C. Ng,[1,‡‡] J. Nishide,[2] T. Numao,[6] A. Otomo,[3,§] J.-M. Poutissou,[6] R. Poutissou,[6] G. Redlinger,[6,§§] T. Sasaki,[4] T. Sato,[3] T. Shinkawa,[3,‖‖] F. C. Shoemaker,[5] R. Soluk,[7] J. R. Stone,[5] R. C. Strand,[1] S. Sugimoto,[3] Y. Tamagawa,[2] C. Witzig,[1] and Y. Yoshimura[3]

(E787 Collaboration)

[1]*Brookhaven National Laboratory, Upton, New York 11973*
[2]*Department of Applied Physics, Fukui University, 3-9-1 Bunkyo, Fukui, Fukui 910-8507, Japan*
[3]*High Energy Accelerator Research Organization (KEK), Oho, Tsukuba, Ibaraki 305-0801, Japan*
[4]*RCNP, Osaka University, 10-1 Mihogaoka, Ibaraki, Osaka 567-0047, Japan*
[5]*Joseph Henry Laboratories, Princeton University, Princeton, New Jersey 08544*
[6]*TRIUMF, 4004 Wesbrook Mall, Vancouver, British Columbia, Canada V6T 2A3*
[7]*Centre for Subatomic Research, University of Alberta, Edmonton, Alberta, Canada T6G 2N5*
[8]*Department of Physics and Astronomy, University of British Columbia, Vancouver, BC, Canada V6T 1Z1*

(Received 1 August 2001; published 14 February 2002)

We have performed a search for the angular-momentum forbidden decay $K^+ \to \pi^+ \gamma$ with the E787 detector at BNL. No events were observed in the π^+ kinematic region around 227 MeV/c. An upper limit on the branching ratio for the decay is determined to be 3.6×10^{-7} at 90% confidence level.

DOI: 10.1103/PhysRevD.65.052009 PACS number(s): 13.25.Es, 11.30.Cp

I. INTRODUCTION

We report on a search for the decay $K^+ \to \pi^+ \gamma$. This is a spin $0 \to 0$ transition with a real photon and is thus forbidden by angular momentum conservation [1]. This decay is also forbidden on gauge invariance grounds [2]. Historically, the absence of $K^+ \to \pi^+ \gamma$ relative to the $K^+ \to \pi^+ \pi^0$ decay ($K_{\pi 2}$) led Dalitz to determine the kaon spin to be zero rather than two or greater [3]. In 1969, a model of strange particles and weak decays predicted this decay at a branching ratio of 2×10^{-4} [4]; the model was later ruled out by an experimental upper limit of 4×10^{-6} at 90% confidence level (C.L.) [5].

No theory of physics beyond the standard model, if it is based on point-particle quantum field theory, allows $K^+ \to \pi^+ \gamma$ decay. Current interest in this decay stems from speculation that an experimental signature of exotic physics, such as a vacuum expectation value of a new vector field [6], nonlocal superstring effects [7], or departures from Lorentz invariance [8], could appear in this decay mode. No specific theoretical prediction or bound on the branching ratio has yet been given.

In previous experiments [5,9] no candidate events were detected. The most recent upper limit of 1.4×10^{-6} at 90% C.L. [9] was established in 1982.

The new search reported here used the E787 detector [10] (see Fig. 1) at the Alternating Gradient Synchrotron (AGS) of Brookhaven National Laboratory (BNL). E787 is a rare kaon-decay experiment studying $K^+ \to \pi^+ \nu \bar{\nu}$ [11] and related decays [12], using kaon decays at rest. $K^+ \to \pi^+ \gamma$ is a two-body decay with a 227-MeV/c π^+ track and a 227-MeV photon emitted directly opposite to it. It is assumed that energy-momentum is conserved or that its violation due to exotic physics is tiny and undetectable in this decay mode.

The main background source is $K_{\pi 2}$ decay with a branching ratio of 0.2116 [13] and a π^+ momentum of 205 MeV/c. The higher energy photon (>125 MeV) from the $\pi^0 \to \gamma\gamma$ decay in $K_{\pi 2}$ tends to be emitted opposite the π^+ track. $K_{\pi 2}$ background events can survive if the π^+ momentum is mismeasured to be too large and at the same time the lower energy photon from the π^0 (or the electron-positron pair from the $\pi^0 \to \gamma e^+ e^-$ decay) is undetected.

*Now at KEK, Oho, Tsukuba, Ibaraki 305-0801, Japan.
†Now at SLAC, Menlo Park, CA 94025.
‡Now at Thomas Jefferson National Accelerator Facility, Newport News, VA 23606.
§Also at Graduate School of Science, The University of Tokyo, Tokyo 113-0033, Japan.
‖Now at Department of Physics, Osaka University, Osaka 560-0043, Japan.
¶Deceased.
**Now at Department of Physics and Astronomy, University of Victoria, Victoria, BC, Canada V8W 3P6.
††Now at Japan Atomic Energy Research Institute, Sayo, Hyogo 679-5198, Japan.
‡‡Also at Department of Physics and Astronomy, State University of New York at Stony Brook, Stony Brook, NY 11794-3800.
§§Now at BNL, Upton, NY 11973.
‖‖Now at the National Defense Academy of Japan, Yokosuka, Kanagawa 239-8686, Japan.

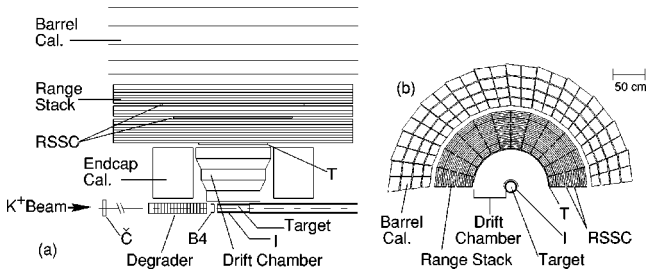

FIG. 1. Schematic sideview (a) and endview (b) showing the upper half of the E787 detector. Č: Čerenkov counter; B4: energy-loss counter; I and T: trigger scintillation counters (I-counters and T-counters); RSSC: range-stack straw-tube tracking chambers.

However, the redundant kinematic measurements and efficient photon detection available in the E787 detector are suited to suppress the $K_{\pi 2}$ and other backgrounds to well below the sensitivity for the signal.

II. DETECTOR

The AGS delivered kaons of about 700 MeV/c to the experiment at a rate of $(4-7)\times 10^6$ per 1.6-s spill. The kaon beam line [14] incorporated two stages of electrostatic particle separation, which reduced the pion contamination to 25% at the entrance of the detector. Kaons were detected and identified by a Čerenkov counter, multi-wire proportional chambers and an energy-loss counter. After being slowed by a BeO degrader, approximately 25% of the incident kaons came to rest in an active stopping target located at the center of the detector. The 12-cm diameter target, which consisted of 0.5-cm square plastic-scintillating fibers, provided initial tracking of the stopping kaon and its decay products.

Particles emanating from kaon decays at rest in the target were measured in a solenoidal spectrometer with a 1.0-T field along the beam axis. The charged decay products passed through a layer of plastic scintillation counters surrounding the target (I-counters) and a cylindrical drift chamber [15], and lost energy in an array of plastic scintillation counters called the Range Stack (RS). The drift chamber provided tracking information for momentum determination from 12 layers of axial anode-wire cells and six layers of thin spiral-strip cathode foils with a total mass of 3×10^{-2} radiation lengths. The RS provided a measurement of range and kinetic energy of the π^+ track which came to rest in it. The radial region between 45.1 cm and 89.6 cm for the RS was segmented into 24 azimuthal sectors and 21 radial layers totaling one radiation length. The RS counters in the first layer (T-counters), which defined the solid angle acceptance for the π^+ track in the RS, were 0.635-cm thick and 52-cm long; the subsequent RS counters in the second layer (RS2-counters) and beyond were 1.905-cm thick and 182-cm long. The RS counter in the sector and layer where the π^+ track came to rest was called the ''stopping counter.'' All the RS counters were read out by phototubes on the upstream and downstream ends. The output pulse shapes were recorded by 500-MHz sampling transient digitizers (TDs) [16], each of which was based on two interleaved 250-MHz 8-bit flash analogue-to-digital converters (ADCs). In addition to providing precise time and energy information for reconstructing the π^+ track, the TDs enabled us to observe the $\pi^+ \rightarrow \mu^+ \nu$ decay at rest in the RS stopping counter. Two layers of straw-tube tracking chambers were embedded in between the 10th and 11th RS layers and between the 14th and 15th RS layers, respectively.

A hermetic calorimeter system, designed primarily to detect photons from $K_{\pi 2}$ and other decays in the $K^+ \rightarrow \pi^+ \nu \bar{\nu}$ study, surrounded the central region. The cylindrical barrel (BL) calorimeter covering about two thirds of the solid angle, and located immediately outside the RS, was used to search for the photon from the $K^+ \rightarrow \pi^+ \gamma$ decay. It consisted of alternating layers of lead (0.1-cm thick) and plastic scintillator (0.5-cm thick) sheets and was segmented azimuthally into 48 sectors whose boundaries were tilted so that the inter-sector gaps did not project back to the target. In each sector, four radial groups of 16, 18, 20 and 21 lead-scintillator layers, respectively with increasing radius, formed BL modules totaling 14.3 radiation lengths. About 29% of the shower energy was deposited in the scintillators. The BL modules, which were 190-cm in length along the beam axis, were read out by phototubes on the upstream and downstream ends, and the outputs were recorded by time-to-digital converters (TDCs) and ADCs. The two endcap calorimeters [17] and additional calorimeters for filling minor openings along the beam direction, as well as any active parts of the detector not hit by the π^+ track, were used for detecting extra particles including photons. The two endcap calorimeters consisted of 143 undoped-CsI crystals, which were read out by fine-mesh phototubes in the 1.0-T field into 500-MHz TDs based on charged coupled devices [18].

III. TRIGGER

The signature of $K^+ \rightarrow \pi^+ \gamma$ in the experiment was a two-body decay of a kaon at rest with a 227-MeV/c π^+ track in the RS and a 227-MeV photon emitted directly opposite to it and observed as a single cluster in the BL calorimeter. The $K^+ \rightarrow \pi^+ \gamma$ trigger required a kaon decay at rest, followed by a π^+ track which came to rest in the RS and a shower cluster in the BL, and no extra particles in the BL, endcap or RS counters.

A kaon was identified in the trigger by a coincidence of hits from the Čerenkov counter, energy-loss counter and target. The timing of the outgoing pion (via the I-counters) was required to be at least 1.5 nsec later than timing of the incoming kaon (via the Čerenkov counter). This online delayed-coincidence requirement guaranteed that the kaon actually decayed at rest, and removed contributions from beam pions that were scattered into the detector and from kaons that decayed in flight after the Čerenkov counter. A single charged track was required to have a coincidence of the hits from the I-counters and from the T-counter and RS2-counter in the same RS sector. The track was also required to penetrate to at least the sixth RS layer in the sector with the coincidence of T-counter and RS2-counter hits or in either of the next two clockwise RS sectors, in order to select positively charged particles. Tracks reaching the outer three RS layers (from the 19th to the 21st layers) were rejected, in

order to suppress the muons from $K^+ \to \mu^+ \nu$ and $K^+ \to \mu^+ \nu \gamma$ decays. A $\pi^+ \to \mu^+ \nu$ decay at rest in the RS stopping counter was identified online, based on the pulse shape information from the TDs on the RS, by an algorithm demanding either a clear double pulse or an RS pulse with an area larger than expected from its height due to the presence of the 4 MeV μ^+ from the π^+ decay. The events that failed the algorithm were rejected, in order to further reduce muon tracks as well as electron tracks. The number of shower clusters in the BL calorimeter with energy above 10 MeV was counted online and was restricted to be one. An event was rejected if the energy observed in the endcap calorimeter was more than 20 MeV or the energy in the RS sectors outside the region of the π^+ track was more than 10 MeV.

The trigger was prescaled by 2450 for taking data simultaneously with the trigger for $K^+ \to \pi^+ \nu \bar{\nu}$. This resulted in a total exposure of kaons entering the target available for the $K^+ \to \pi^+ \gamma$ search to be 6.7×10^8. A total of 1.6×10^6 events met the trigger requirements. Most of them were due to $K_{\pi 2}$.

IV. OFFLINE ANALYSIS

A. Event reconstruction

In the offline analysis, the momentum (P), the range (equivalent cm of plastic scintillator, R) and the kinetic energy (E) of the π^+ track were reconstructed with the target, drift chamber and RS information. The momentum was determined by correcting the measured momentum in the drift chamber for the energy loss suffered by the π^+ track with the observed track length in the target. The range was calculated from the track lengths in the target and in the RS. The kinetic energy was determined by adding up the energy deposits of the π^+ track in the scintillators of the target and the RS, taking account of the losses in inactive materials such as wrapping and chamber components. The RS energy calibration was done for the upstream and downstream end separately, using the energy loss in each counter of muons from $K^+ \to \mu^+ \nu$ decay. The kinematic resolutions (rms) were $\Delta P = 2.6$ MeV/c, $\Delta R = 1.28$ cm and $\Delta E = 3.8$ MeV.

The timing, energy (E_γ) and direction of the photon were determined from reconstruction of the hits in the BL calorimeter and the kaon decay vertex position in the target. The π^+ track in the RS defined the event time reference, and photons from $K_{\pi 2}$ decay were used to calibrate the BL hit time. The energy calibration of the BL hits was performed using the energy depositions from cosmic rays, and was verified by reconstructing the energy of the π^0 in $K_{\pi 2}$ decay. The z position (along the beam axis) of the BL hits was measured with TDC and ADC information from phototubes on both ends of the BL modules, and was used in conjunction with target information to determine the polar angle of the photon. The energy resolution of the BL calorimeter was $\Delta E_\gamma / E_\gamma = 6\% / \sqrt{E_\gamma}$ (E_γ in GeV). The resolutions of azimuthal and polar opening angles between the photon and the π^+ track, $\phi_{\pi^+ \gamma}$ and $\theta_{\pi^+ \gamma}$, were determined to be $\Delta \phi_{\pi^+ \gamma} = 2.2°$ and $\Delta \theta_{\pi^+ \gamma} = 3.9°$, respectively.

B. Primary cuts

The following selection criteria (''cuts''), called the primary cuts in the analysis, were imposed on the events that were successfully reconstructed.

A stopping-layer cut accepted only events whose π^+ track came to rest in the RS layers beyond the inner RS tracking chamber (from the 11th to the 18th layers) for analysis. This cut was imposed to ensure that the range measurement included positions determined by the RS tracking chambers.

Taking into consideration the limited energy resolution and segmentation of the BL calorimeter, the cuts imposed on the energy and direction of the photon in the BL were relatively loose: $E_\gamma \geqslant 120$ MeV, $|\phi_{\pi^+ \gamma}| \geqslant 165°$ and $\theta_{\pi^+ \gamma} \geqslant 165°$. A coincidence cut ($\pm$ 2 ns) between the times of the photon and the π^+ track was imposed. This cut greatly reduced the occurrence of photon candidates due to accidental hits. Events in which the photon cluster in the BL showed associated activity in the neighboring RS sectors were rejected by a ''RS preshower'' cut, so that only those events whose total photon shower energy was deposited in the BL calorimeter were accepted.

To remove events triggered by kaon decays in flight or by multiple beam particles into the detector, an offline delayed-coincidence cut requiring >2 ns between the pion time and the kaon time measured in the target, and cuts on the timing and energy of the hits recorded in the Čerenkov counter, proportional chambers, energy-loss counter and target were imposed.

A double-pulse fit to the pulse shape recorded in the RS stopping counter was made offline to identify pions with $\pi^+ \to \mu^+ \nu$ decay at rest; this cut removed contamination from $K^+ \to \mu^+ \nu$, $K^+ \to \mu^+ \nu \gamma$, $K^+ \to \mu^+ \pi^0 \nu$ and $K^+ \to e^+ \pi^0 \nu$ decays, as well as $K_{\pi 2}$ decays whose π^+ decayed in flight before it came to rest in the RS.

C. $\pi\gamma$ sample and $\pi\pi^0$ sample

The following two data sets were made from the events that survived the primary cuts.

The set of events with $218 \leqslant P \leqslant 234$ MeV/c was identified as the ''$\pi\gamma$ sample.'' The $K^+ \to \pi^+ \gamma$ signal region[1] was further specified as the subset of the $\pi\gamma$ sample with $35.5 \leqslant R \leqslant 40.0$ cm and $120 \leqslant E \leqslant 135$ MeV. These cuts ensured that the π^+ momentum, range and kinetic energy were consistent with those of the π^+ track from the $K^+ \to \pi^+ \gamma$ decay: 227 MeV/c, 38.5 cm and 127 MeV, respectively.

The set of events that were collected by the same $K^+ \to \pi^+ \gamma$ trigger and whose π^+ momentum and range were rather consistent with $K_{\pi 2}$ decay ($197.5 \leqslant P \leqslant 212.5$ MeV/c and $27.0 \leqslant R \leqslant 35.0$ cm) was identified as the ''$\pi\pi^0$ sample.'' This sample was rich in $K_{\pi 2}$ back-

[1]This signal region is the same as that for the search for $K^+ \to \pi^+ X^0$ decay in [11], where X^0 is a neutral weakly interacting massless particle [19] and the π^+ momentum, 227 MeV/c, is identical to the momentum for $K^+ \to \pi^+ \gamma$.

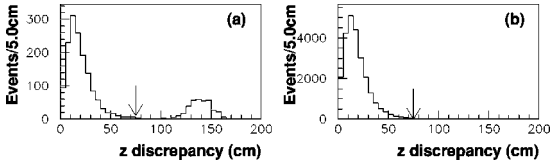

FIG. 2. (a) z discrepancy distribution of the BL clusters in the subset of the $\pi\pi^0$ sample with all photon veto cuts imposed. (b) z discrepancy distribution of the BL clusters when the other photon from the π^0 decay in $K_{\pi 2}$ was detected outside of the cluster. Events above the arrow in each distribution corresponded to multiple photon hits and were rejected by the cut at 75 cm.

ground, and was used for evaluating the rejections of cuts in the background studies.

V. BACKGROUND STUDIES

After the primary cuts were imposed, the remaining background events were mostly from $K_{\pi 2}$ decay. This background was due to the disappearance of the softer of the two photons from π^0, either through inefficiency due to very narrow gaps between counters, inactive material, etc. (''photon detection inefficiency'') or through overlap with the charged track (''overlapping photon''). Both types were studied from the data by establishing two independent sets of offline cuts for each type; one set consisted of the cuts on the π^+ momentum, range and kinetic energy, and the other set consisted of ''photon veto cuts'' (for photon detection inefficiency) or ''dE/dx cuts'' (for overlapping photon), as explained in the next subsections. In these studies we selected events in the $\pi\pi^0$ sample or inverted at least one of these cuts on the events in the $\pi\gamma$ sample, in order to enhance the background collected by the $K^+\rightarrow\pi^+\gamma$ trigger as well as to prevent candidate events from being examined before the background studies were completed. In order to avoid contamination from other background sources, all the offline cuts except for those being established were imposed on the data.[2]

A. Photon detection inefficiency

In the offline analysis, photon shower activity was identified in the various subsystems, including the BL calorimeter and the RS, as hits in the counters in coincidence with the π^+ track within a few ns and with energy above a low threshold (typically $\sim$1 MeV). Events with extra activity not associated with the π^+ and the candidate signal photon were rejected by the offline photon veto cut of each subsystem.

If two photons from a π^0 hit the same or adjacent BL modules, they form a single high-energy BL cluster opposite the π^+ track and can mimic $K^+\rightarrow\pi^+\gamma$ decay. In such cases, due to the kinematics of $K_{\pi 2}$ and subsequent $\pi^0\rightarrow\gamma\gamma$ decays, the two photons must hit the modules at different z positions along the beam axis. The coincidence cut between the times of the photon and the π^+ track, already imposed as a primary cut, reduced the number of events with two photons in the same BL module, because the mean of the arrival times of the scintillation light at the upstream and downstream ends of the BL module was significantly earlier than that of a single photon hit. Furthermore, the BL hits in the cluster were examined and the maximum discrepancy among the z-position measurements obtained from TDC and ADC information was determined. Figure 2(a) shows the z discrepancy distribution of the BL clusters in the subset of the $\pi\pi^0$ sample that survived all photon veto cuts. Comparing this to Fig. 2(b), which shows the z discrepancy distribution of the BL clusters when the other photon from the π^0 decay in $K_{\pi 2}$ was detected outside of the cluster, the events with a large discrepancy in Fig. 2(a) clearly represent the case when two photons hit adjacent BL modules. A ''BL cluster'' cut was therefore employed to reject an event if the discrepancy was more than 75 cm.

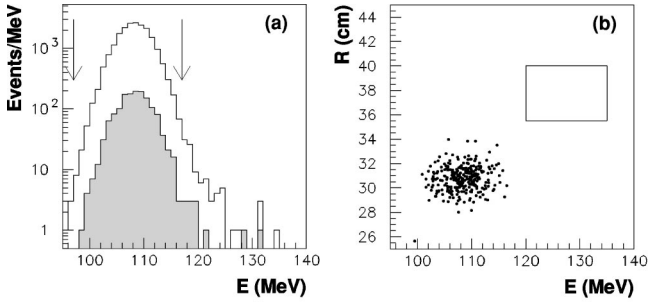

FIG. 3. (a) Kinetic energy distribution of the $\pi\pi^0$ sample. The unhatched and hatched histograms represent the distributions before and after the photon veto cuts are imposed, respectively. The region between the arrows indicates the $K_{\pi 2}$ region. (b) Range versus kinetic energy plot of the events in the subset of the $\pi\gamma$ sample tagged by the inverted photon veto cuts. The box indicates the $K^+\rightarrow\pi^+\gamma$ signal region. dE/dx cuts were imposed on both the $\pi\pi^0$ sample in (a) and the $\pi\gamma$ sample in (b) in advance.

To evaluate the background rejection of the offline photon veto cuts including the BL cluster cut, the subset of the $\pi\pi^0$ sample whose π^+ kinetic energy was also consistent with $K_{\pi 2}$ decay ($97\leqslant E\leqslant 117$ MeV) was examined. By imposing the photon veto cuts on this subset, the background rejection of these cuts was measured to be 13.8 as shown in Fig. 3(a). Then, in the subset of the $\pi\gamma$ sample that failed at least one of the offline photon veto cuts, the kinematic distributions of $K_{\pi 2}$ background events[3] was studied. The π^+ range versus kinetic energy plot of these events is shown in Fig. 3(b); there are no events in the $K^+\rightarrow\pi^+\gamma$ signal region, and 287 events are consistent with $K_{\pi 2}$ decay in range and kinetic energy. This indicates that there are no mismeasured tracks in or around the signal region, and a further background reduction by 13.8 is expected, assuming the π^+ range and kinetic-energy cuts and the photon veto cuts are independent.

[2]For example, in the study of the photon detection inefficiency, dE/dx cuts were imposed on both the $\pi\pi^0$ sample and the $\pi\gamma$ sample in advance.

[3]The $\pi\gamma$ sample was made by choosing the events that survived the π^+ momentum cut $218\leqslant P\leqslant 234$ MeV/c.

In estimating the background level of $K_{\pi 2}$ in a specific π^+ region in range and kinetic energy, the number of events in the region in Fig. 3(b) was divided by the rejection (13.8) minus 1.[4] The number of events in the signal region in Fig. 3(b) was taken to be <2.44 events at 90% C.L. [13,20] instead of zero. The background levels of $K_{\pi 2}$ in the signal region and in the $K_{\pi 2}$ region were therefore estimated to be <0.19 events at 90% C.L. and 22.4 ± 1.3 events, respectively.

Figure 3(b) indicates that no correlation between the π^+ range and kinetic energy is visible in the $K_{\pi 2}$ background events at the current sensitivity of the search. If we further added the assumption that the π^+ range and kinetic energy measurements were indeed not correlated, the background level of $K_{\pi 2}$ in the signal region was estimated to be <0.0007 events at 90% C.L.[5]

B. Overlapping photon

The above background study could possibly be confounded by $K_{\pi 2}$ events in which the shower of the lower energy photon from the π^0 overlapped some of the counters hit by the π^+ track. The reconstructed kinetic energy of such tracks could be incorrectly measured due to additional energy deposited in the scintillators by the overlapping photon. A set of dE/dx cuts, which checked the consistency between the measured energy and range in each of the RS counters, was therefore employed to reject this type of background. Events with a RS counter in which the measured energy was larger than expected from the reconstructed range in that counter were rejected by the dE/dx cuts.

To evaluate the background rejection of the dE/dx cuts, we selected events in the $\pi\pi^0$ sample whose π^+ kinetic energy was larger than that from $K_{\pi 2}$ decay and was in the signal region for $K^+ \to \pi^+ \gamma$ ($120 \leqslant E \leqslant 135$ MeV). By imposing the dE/dx cuts on this subset, the background rejection of these cuts was measured to be 36.3 as shown in Fig. 4(a). From the subset of the $\pi\gamma$ sample that failed at least one of the dE/dx cuts, the π^+ range versus kinetic energy plot is shown in Fig. 4(b); again no mismeasured tracks are in or around the $K^+ \to \pi^+ \gamma$ signal region. The background level of $K_{\pi 2}$ in the signal region was estimated to be <0.07 events at 90% C.L.[6] The estimate is limited by statistics.

C. $K^+ \to \pi^+ \gamma\gamma$ decay

For $K^+ \to \pi^+ \gamma\gamma$ decay in the π^+ momentum region greater than 215 MeV/c, a 90% C.L. upper limit of 5.0×10^{-7} on the branching ratio has been established [21] (assuming a phase-space kinematic distribution). Taking into account further suppression by the trigger requirements, offline photon veto cuts and dE/dx cuts to the $K^+ \to \pi^+ \gamma\gamma$ decay, its contribution to the $K^+ \to \pi^+ \gamma$ search is negligible at the current sensitivity.

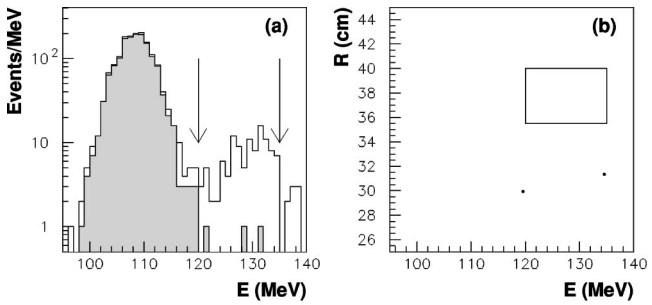

FIG. 4. (a) Kinetic energy distribution of the $\pi\pi^0$ sample. The unhatched and hatched histograms represent the distributions before and after the dE/dx cuts are imposed, respectively. The region between the arrows indicates the signal region for $K^+ \to \pi^+ \gamma$. (b) Range versus kinetic energy plot of the events in the subset of the $\pi\gamma$ sample tagged by the inverted dE/dx cuts. The box indicates the $K^+ \to \pi^+ \gamma$ signal region. Photon veto cuts were imposed on both the $\pi\pi^0$ sample in (a) and the $\pi\gamma$ sample in (b) in advance.

VI. RESULT

A. Events in the signal region

Figure 5 shows the π^+ range versus kinetic energy plot of the events that survived all analysis cuts. No events were observed in the signal region. The group of 20 events around $E = 108$ MeV was due to the $K_{\pi 2}$ background and was consistent with the 22.4 ± 1.3 events expected from the estimate of the photon detection inefficiency discussed above.

B. Sensitivity

The single-event sensitivity for $K^+ \to \pi^+ \gamma$ decay in this search was obtained by normalizing to the number of $K_{\pi 2}$ events collected by the $K^+ \to \pi^+ \gamma$ trigger. For the $K_{\pi 2}$ events, the π^+ track in the RS and the higher energy photon in the BL calorimeter were reconstructed, and the offline analysis cuts of the $K^+ \to \pi^+ \gamma$ search except for those sensitive to the photons from π^0 (the RS preshower cut, photon veto cuts, dE/dx cuts and target energy cuts) were imposed. The number of events whose π^+ momentum, range and kinetic energy were consistent with $K_{\pi 2}$ decay was 3.62×10^5.

Acceptance factors were determined from the sample generated by Monte Carlo simulation and from the data samples of $K_{\pi 2}$ decays,[7] $K^+ \to \mu^+ \nu$ decays and scattered beam pions, which were accumulated by calibration triggers simultaneous

[4]The number of events should be divided by the tagging efficiency of the inverted photon veto cuts ϵ, and by the rejection of the photon veto cuts R. Since ϵ is equal to $1 - 1/R$, the estimate is equivalent to the number of events divided by R minus 1.

[5]The number of events that survived the π^+ range cut, <2.44 events at 90% C.L. instead of zero, was divided by the rejection of the π^+ kinetic-energy cut [taken to be 287 from the number of events in Fig. 3(b)] minus 1, and by the rejection of the photon veto cuts (13.8) minus 1.

[6]The number of events in the signal region in Fig. 4(b), <2.44 events at 90% C.L. instead of zero, was divided by the rejection of the dE/dx cuts (36.3) minus 1.

[7]The sample of $K_{\pi 2}$ decays for measuring acceptance factors in this subsection was accumulated by a calibration trigger that removed the requirements on the shower and visible energy in the BL, endcap and RS counters from the $K^+ \to \pi^+ \gamma$ trigger.

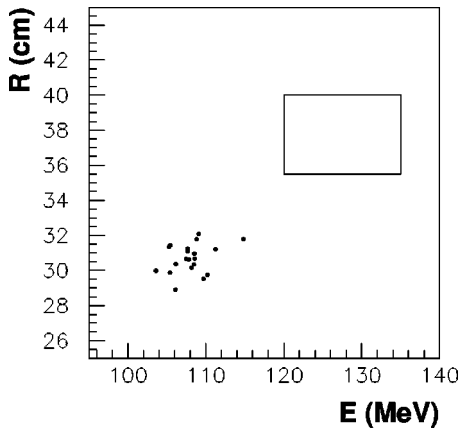

FIG. 5. Range versus kinetic energy plot of the events with all analysis cuts imposed. The box indicates the signal region for $K^+ \to \pi^+ \gamma$.

to the collection of signal candidates. Many systematic uncertainties in the measurement of the acceptance factors for $K^+ \to \pi^+ \gamma$ and $K_{\pi 2}$ (e.g., the fraction of kaons entering the target that decayed at rest, ~ 0.72) canceled in taking the ratio of acceptances of these decay modes. The factors are summarized in Table I.

The acceptance factors of the π^+ reconstruction cuts (including the online requirements in the trigger) and the π^+ kinematic fiducial cuts specifying the signal region and the $K_{\pi 2}$ region (including the stopping-layer cut) were estimated primarily from Monte Carlo simulation. The loss when the π^+ track underwent nuclear interaction or decayed in flight before it came to rest in the RS was estimated by comparing Monte Carlo simulations with these effects turned on and off. The π^+ acceptance factors of the online and offline cuts selecting the $\pi^+ \to \mu^+ \nu$ decay at rest in the RS stopping counter and of the dE/dx cuts were measured from the sample of scattered beam pions that satisfied the fiducial cuts. The acceptance factor of the target energy cuts was measured from the π^+ tracks in the sample of $K_{\pi 2}$ decays tagged by the conversion of both photons from the $\pi^0 \to \gamma\gamma$ decay in the BL calorimeter, in order to avoid contamination from shower energy due to photon conversion in the target. The acceptance factors of the online and offline delayed-coincidence cuts and the cuts on the Čerenkov counter, proportional chambers, energy-loss counter and target were measured from the sample of $K^+ \to \mu^+ \nu$ decays; since these cuts were not related to the kinematic values of π^+, these factors were assumed to be the same for both the $K^+ \to \pi^+ \gamma$ and $K_{\pi 2}$ decays.

The acceptance factors of the γ reconstruction and fiducial cuts were estimated from Monte Carlo simulation. The acceptance loss of the $K_{\pi 2}$ events due to the trigger requirements on the shower and visible energy in the BL, endcap and RS counters (''online photon veto cuts'') was measured from the sample of $K_{\pi 2}$ decays. The acceptance loss of $K^+ \to \pi^+ \gamma$ due to the online and offline photon veto cuts and the RS preshower cut, which could detect a part of the shower from the 227-MeV photon in the $K^+ \to \pi^+ \gamma$ decay, must be taken into account. Since a data sample of 227-MeV photons from kaon decays at rest was not available, the acceptance factor was estimated from studies that compared the performance of these cuts on the photons in Monte Carlo simulation and on the sample of $K_{\pi 2}$ decays. The acceptance loss by the accidental hits in the detector subsystems was measured from the sample of $K^+ \to \mu^+ \nu$ decays. Acceptance losses due to the cuts on the BL hits in the cluster (the coincidence cut between the times of the photon and the π^+ track and the BL cluster cut) were confirmed to be negligible from the photons in the sample of $K_{\pi 2}$ decays.

TABLE I. Acceptance factors for $K^+ \to \pi^+ \gamma$ and $K^+ \to \pi^+ \pi^0$, and the samples used to determine them. ''MC,'' ''$K_{\pi 2}$,'' ''$K_{\mu 2}$'' and ''π_{scat}'' mean the sample generated by Monte Carlo simulation and the data samples of $K^+ \to \pi^+ \pi^0$ decays, $K^+ \to \mu^+ \nu$ decays and scattered beam pions accumulated by calibration triggers, respectively. The dE/dx cuts, target energy cuts, offline photon veto cuts and RS preshower cut are not imposed on $K^+ \to \pi^+ \pi^0$. (*) not imposed.

Acceptance factors	$\pi^+ \gamma$	$\pi^+ \pi^0$	Samples
π^+ reconstruction cuts	0.399	0.400	MC, $K_{\mu 2}$
π^+ fiducial cuts	0.830	0.694	MC
π^+ stop without nuclear interaction or decay-in-flight	0.477	0.586	MC
Transient digitizer ($\pi^+ \to \mu^+ \nu$) cuts	0.553	0.592	π_{scat}
dE/dx cuts	0.878	ni*	π_{scat}
Target energy cuts	0.924	ni*	$K_{\pi 2}$
Other cuts on beam and target	0.606	0.606	$K_{\mu 2}$
γ reconstruction and fiducial cuts	0.693	0.232	MC
Online photon veto cuts to $\pi^+ \pi^0$	ni*	0.264	$K_{\pi 2}$
Online and offline photon veto cuts and RS preshower cut to the photon from $\pi^+ \gamma$	0.482	ni*	MC, $K_{\pi 2}$, $K_{\mu 2}$
Total acceptance	0.0143	0.00357	

With the total acceptances for $K^+ \to \pi^+ \gamma$ (0.0143) and for $K^+ \to \pi^+ \pi^0$ (0.00357) in Table I, the number of surviving $K_{\pi 2}$ events (3.62×10^5) and the $K_{\pi 2}$ branching ratio (0.2116), the single-event sensitivity for $K^+ \to \pi^+ \gamma$ was $(1.46 \pm 0.09) \times 10^{-7}$, which is four times better than the sensitivity achieved in [9]. The main source of the error (6%) was due to the systematic uncertainty in the acceptance loss of the 227-MeV photon from $K^+ \to \pi^+ \gamma$ due to the online and offline photon veto cuts and the RS preshower cut.

In order to verify that the sensitivity for $K^+ \to \pi^+ \gamma$ obtained from the ratio to $K_{\pi 2}$ decay was correct, a branching ratio for $K_{\pi 2}$ relative to the sample of $K^+ \to \mu^+ \nu$ decays was measured and the result deviated by $+6\%$ from the known ratio of the $K_{\pi 2}$ and $K^+ \to \mu^+ \nu$ branching ratios. We have conservatively assigned the shift to be an additional systematic uncertainty in the acceptance of the π^+ track, most probably due to the uncertainty in π^+ nuclear interaction. The total estimated systematic uncertainty in this search is therefore 8.5%.

VII. CONCLUSION

A search for the decay $K^+ \to \pi^+ \gamma$ was performed with the E787 detector at BNL as a test of angular momentum conservation in particle physics. Since no events were observed in the signal region, in the absence of background and taking 2.44 events instead of zero according to the unified approach [13,20], we set a 90% C.L. upper limit 3.6×10^{-7} on the branching ratio for $K^+ \to \pi^+ \gamma$ decay. The systematic uncertainty was not taken into consideration in deriving the limit.

The current search is statistically limited, and there are good prospects to improve the sensitivity further. A new experiment E949 [22], which will continue the study of the $K^+ \to \pi^+ \nu \bar{\nu}$ decay at BNL, can yield further gains by virtue of a larger kaon exposure, trigger optimization and improved photon detection capability.

ACKNOWLEDGMENTS

We gratefully acknowledge the dedicated effort of the technical staff supporting this experiment and of the Brookhaven Collider-Accelerator Department. This research was supported in part by the U.S. Department of Energy under Contracts No. DE-AC02-98CH10886, W-7405-ENG-36, and grant DE-FG02-91ER40671, by the Ministry of Education, Culture, Sports, Science and Technology of Japan through the Japan-U.S. Cooperative Research Program in High Energy Physics and under the Grant-in-Aids for Scientific Research, for Encouragement of Young Scientists and the JSPS, and by the Natural Sciences and Engineering Research Council and the National Research Council of Canada.

[1] E.g., K. Nishijima, *Fundamental Particles* (Benjamin, New York, 1963), Sec. 2.12; J.J.Sakurai, *Invariant Principles and Elementary Particles* (Princeton University Press, Princeton, NJ, 1964), Sec. 2.4.

[2] S. Ôneda, S. Sasaki, and S. Ozaki, Prog. Theor. Phys. **5**, 165 (1950); H. Fukuda, S. Hayakawa, and Y. Miyamoto, *ibid.* **5**, 352 (1950).

[3] R.H. Dalitz, Phys. Rev. **99**, 915 (1955); Proc. Phys. Soc., London, Sect. A **69**, 527 (1956).

[4] F. Selleri, Nuovo Cimento A **57**, 678 (1968); **60**, 291 (1969).

[5] J.H. Klems *et al.*, Phys. Rev. Lett. **25**, 473 (1970); Phys. Rev. D **4**, 66 (1971).

[6] G.L. Kane, in *Proceedings of the 9th European Symposium on Proton-Antiproton Interactions and Fundamental Symmetries*, Mainz, Germany, edited by K. Kleinknecht and E. Klempt [Nucl. Phys. B (Proc. Suppl.) **8**, 469 (1989)].

[7] G.L. Kane, Phys. Today **50**(2), 40 (1997).

[8] S. Coleman and S.L. Glashow, Phys. Rev. D **59**, 116008 (1999).

[9] Y. Asano *et al.*, Phys. Lett. **113B**, 195 (1982).

[10] M.S. Atiya *et al.*, Nucl. Instrum. Methods Phys. Res. A **321**, 129 (1992).

[11] S. Adler *et al.*, Phys. Rev. Lett. **79**, 2204 (1997); S. Adler *et al.*, *ibid.* **84**, 3768 (2000).

[12] S. Adler *et al.*, Phys. Rev. Lett. **85**, 2256 (2000); S. Adler *et al.*, *ibid.* **85**, 4856 (2000); S. Adler *et al.*, Phys. Rev. D **63**, 032004 (2001).

[13] Particle Data Group, D.E. Groom *et al.*, Eur. Phys. J. C **15**, 1 (2000).

[14] J. Doornbos *et al.*, Nucl. Instrum. Methods Phys. Res. A **444**, 546 (2000).

[15] E.W. Blackmore *et al.*, Nucl. Instrum. Methods Phys. Res. A **404**, 295 (1998).

[16] M.S. Atiya *et al.*, Nucl. Instrum. Methods Phys. Res. A **279**, 180 (1989).

[17] I-H. Chiang *et al.*, IEEE Trans. Nucl. Sci. **NS-42**, 394 (1995); T.K. Komatsubara *et al.*, Nucl. Instrum. Methods Phys. Res. A **404**, 315 (1998).

[18] D.A. Bryman *et al.*, Nucl. Instrum. Methods Phys. Res. A **396**, 394 (1997).

[19] F. Wilczek, Phys. Rev. Lett. **49**, 1549 (1982).

[20] G.J. Feldman and R.D. Cousins, Phys. Rev. D **57**, 3873 (1998).

[21] P. Kitching *et al.*, Phys. Rev. Lett. **79**, 4079 (1997).

[22] B. Bassalleck *et al.*, E949 Proposal, BNL-67247, TRI-PP-00-06, 1999. The information on E949 is available through http://www.phy.bnl.gov/e949/.